

Using FMRI and FNIRS for localization and monitoring of visual cortex activities

Nasser H. Kashou, *Member, IEEE*, Ronald Xu, *Member, IEEE*, Cynthia J. Roberts, *Member, IEEE*
and Lawrence E. Leguire

Abstract— The purpose of this study was to design a near infrared spectroscopy (NIRS) sensor head to continuously monitor visual cortex activation. Visual cortex activation regions as a result of eye movements were localized using functional magnetic resonance imaging (FMRI). Once the region was determined we placed the NIRS sensor head on that region and emulated the same task performed in the FMRI experiment. The eye movement chosen for our current validation study was saccades. One subject was instructed to move their eyes in a saccadic fashion for 30 seconds then fixate for 30 seconds. We were able to see changes in oxyhemoglobin and deoxyhemoglobin using the NIRS design. These preliminary results suggest that NIRS can be used as a monitoring tool, guided by FMRI in patients who may have visual disorders.

I. INTRODUCTION

Studying brain functional activities is an area that is experiencing rapid growth in the field of biomedical imaging. Magnetic resonance imaging (MRI) is the most common modality used in functional imaging. However, just like with any other modality, it has some drawbacks, including the lack of portability and expense. That is why functional researchers are turning to new modalities either to simultaneously use or run standalone. Near infrared spectroscopy (NIRS) is one of these modalities because of its high temporal resolution. Currently there have been and are efforts to combine NIR with MRI [1]-[6]. We introduce the concept of continuous monitoring of the visual cortex subsequent to an FMRI scan rather than simultaneously.

A. Clinical Significance

Functional near-infrared spectroscopy (FNIRS) offers the ability to monitor brain activation by measuring changes in the concentration of oxy- and deoxy-hemoglobin (Hb) by their different spectra in the near-infrared range [7]-[10]. NIRS may be useful in detecting visual dysfunction

objectively and noninvasively in patients with visual disturbance. Specifically, Miki et al. [11] demonstrated that a decreased activation of the visual cortex in patients with optic neuritis, which can be seen with NIRS. Also, Wilcox et al. [12] has studied the relationship between object processing and brain function in human infants, and observed neural activation in the primary visual cortex and the inferior temporal cortex. However, other than these few studies no thorough studies have been made related to the visual cortex and specifically visual disorders. Thus, we combined both FMRI and FNIRS technology to first localize the regions of the cortex that are normally highly activated in the subject, and then to repeat the same task using FNIRS by properly placing the sensor on the location determined by the FMRI scan.

II. TECHNOLOGY REVIEW

A. Near Infrared Light (NIR)

For more than two decades, the single channel measurement technique of NIR spectroscopy has been successfully used to measure the hemodynamic response to brain activity in both adults and neonates [13]-[14]. More recent studies using the multi channel NIRS technique, NIR optical topography (OT), have improved spatial and temporal resolution in both adults [15] and infants [16].

Near infrared light ranges from 600-950nm and is strongly absorbed by two chromophores, namely, oxyhemoglobin (HbO) and deoxyhemoglobin (Hb). As a result of this interaction, the modified Beer-Lambert Law (MBLL), seen in (1), can be used to quantify changes in chromophore concentrations [17]-[18].

$$\Delta OD = -\ln(I_{final}/I_{initial}) = \epsilon \Delta C L B \quad (1)$$

where $\Delta OD = OD_{final} - OD_{initial}$ is the change in optical density, I_{final} and $I_{initial}$ are the measured intensities before and after the concentration of the chromophores change, ΔC . L is the distance between incident light and detected light, ϵ is the extinction coefficient, and B is the differential path-length factor (DPF). The general one chromophore equation can be further expanded for brain functional monitoring applications where two chromophores need to be monitored, yielding (2).

$$\Delta OD^\lambda = (\epsilon^\lambda_{HbO} \Delta[HbO] + \epsilon^\lambda_{Hb} \Delta[Hb]) B^\lambda L \quad (2)$$

Manuscript received April 16, 2007.

N. H. Kashou is with the Biomedical Engineering Department, The Ohio State University, Columbus, OH 43210 USA (phone: 614-292-1831; fax: 614-292-7301; e-mail: nhkashou@ieee.org).

R. Xu is with Biomedical Engineering Department, The Ohio State University, Columbus, OH 43210 USA (e-mail: xu.202@osu.edu).

C. J. Roberts is with the Biomedical Engineering Department and the Ophthalmology Department, The Ohio State University, Columbus, OH 43210 USA (e-mail: roberts.8@osu.edu).

L. E. Leguire is with the Ophthalmology Department, Childrens Hospital, Columbus, OH 43205 USA; The Biomedical Engineering Department and the Ophthalmology Department, The Ohio State University, Columbus, OH 43210 USA (e-mail: leguirel@chi.osu.edu).

where λ indicates particular wavelength. After rearranging the mathematical terms the concentration changes can now be computed by measuring the change in optical density at two different wavelengths as seen in (3) and (4).

$$\Delta[\text{Hb}] = \frac{[(\epsilon_{\text{HbO}}^{\lambda_2} (\Delta\text{OD}^{\lambda_1} / B^{\lambda_1})) - (\epsilon_{\text{HbO}}^{\lambda_1} (\Delta\text{OD}^{\lambda_2} / B^{\lambda_2}))]}{[(\epsilon_{\text{Hb}}^{\lambda_1} \epsilon_{\text{HbO}}^{\lambda_2} - \epsilon_{\text{Hb}}^{\lambda_2} \epsilon_{\text{HbO}}^{\lambda_1})L]} \quad (3)$$

$$\Delta[\text{HbO}] = \frac{[(\epsilon_{\text{HbO}}^{\lambda_1} (\Delta\text{OD}^{\lambda_2} / B^{\lambda_2})) - (\epsilon_{\text{HbO}}^{\lambda_2} (\Delta\text{OD}^{\lambda_1} / B^{\lambda_1}))]}{[(\epsilon_{\text{Hb}}^{\lambda_1} \epsilon_{\text{HbO}}^{\lambda_2} - \epsilon_{\text{Hb}}^{\lambda_2} \epsilon_{\text{HbO}}^{\lambda_1})L]} \quad (4)$$

The basic process is now to propagate two near infrared wavelengths through the tissue, one which is more strongly absorbed by oxyhemoglobin and the other by deoxyhemoglobin at two different time periods and take the difference of these concentrations. In this case all the other variables in (3) and (4) are defined by the design. This is possibly the simplest way to do these measurements.

B. NIR Systems

Time domain (TD), frequency domain (FD), and continuous-wave (CW) systems are currently being used to solve the above implementation of NIRS [19]. TD systems [20]-[24] introduce into tissue light impulses on the order of picoseconds which after passing through different layers such as skin, skull, cerebrospinal fluid (CSF), and brain become broadened and attenuated [19]. The output of this pulse after being transmitted through the highly scattered medium is known as the temporal point spread function (TPSF) [20]. An advantage of TD systems over the latter two is that theoretically it can obtain the highest spatial resolution and can accurately determine absorption and scattering [19]. The disadvantages include lower temporal resolution as a direct result of trying to achieve an adequate signal to noise ratio, large dimensions, high cost due to the necessary ultrafast lasers, as well as the requirement to mechanically stabilize the instrument [25].

In FD systems, [26]-[29] the light source is continuously operating, but is amplitude modulated at frequencies on the order of tens to hundreds of megahertz. FD systems have the advantage of achieving higher temporal resolution than TD systems. One disadvantage is the noise in the measurements of scattering effects [19].

In CW systems, [30]-[33] light sources emit light continuously at constant amplitude or modulated frequencies not higher than a few tens of kilohertz [19]. The most highly developed application of CW imaging technology is the study of hemodynamic and oxygenation changes in superficial tissues, and of the outer (cortical) regions of the brain in particular using optical topography [34]. An advantage of CW systems over the other two is their cost. However, the main disadvantage is the inability to uniquely quantify the effects of light scattering and absorption [35]. Other disadvantages are that intensity measurements are far more sensitive to the optical properties of tissues at or immediately below the surface than to the properties of localized regions deeper within the tissue [34]. This is due to the characteristic 'banana' shape of the volume of tissue over

which the measurement is sensitive, which is narrow near the source and detector and very broad in the middle [36]-[37]. Also the detected intensity is highly dependent on surface coupling, meaning if an optical fiber is moved slightly or pressed more firmly on the skin then it can result in a very large change in measurement [34].

III. EXPERIMENTAL DESIGN

A. FMRI Scanning Parameters

FMRI was performed with a 3.0T GE Medical Systems Signa Excite and the BOLD sensitive T2* weighted echo-planar (EPI) sequence [38] using an 8 channel array RF coil. Scanning protocol included a screening brain MR scan, including sagittal T1-weighted and axial T2-weighted scans, to exclude any anatomic brain abnormality (e.g., Arnold – Chiari malformation) [39]. The locations of activation and deactivation clusters were defined with respect to the Montreal Neurological Institute (MNI) coordinates and anatomical landmarks [40]-[42]. These sites were identified with the Talairach and Tournoux [43] atlas. The FMRI acquisition parameters were: $TE = 35$ ms; $TR = 1.5$ s; flip angle = 90° single shot; full k -space; 64×64 acquisition matrix with a field of view (FOV) = 24 cm, generating an in-plane resolution of 3.75 mm^2 with a max total of 23 axial slices. A total of 120 volumes (time points) were acquired. For anatomic imaging, we used a three-dimensional volume spoiled gradient-echo pulse sequence (0.469 mm^2) in the axial plane and obtained 1.3 mm thick slices.

B. FMRI Data Analysis

Data analysis was carried out using FEAT (FMRI Expert Analysis Tool) Version 5.4 (FMRIB Software Library, www.fmrib.ox.ac.uk/fsl). Slice-timing correction using Fourier-space time-series phase-shifting, motion correction using MCFLIRT [44], mean-based intensity normalization of all volumes by the same factor, and highpass temporal filtering (Gaussian-weighted LSF straight line fitting, with $\sigma = 30$ s) were applied as pre-statistics processing. No spatial smoothing of the data was performed. Post processing motion correction included voxel displacements: absolute (each time point with respect to the reference image = 0.14mm) and relative (each time point with respect to the previous image = 0.04mm). Independent Component Analysis (ICA)-based exploratory data analysis was carried out using MELODIC [45], in order to investigate the possible presence of activation or unexpected artifacts. Time-series statistical analysis was carried out using FILM with local autocorrelation correction [46]. Z (Gaussianized T/F) statistic images were thresholded using clusters determined by an average $Z > 5.1$ and a (corrected) cluster significance threshold of $P < 0.05$ [47]-[49]. Registration to high resolution and/or standard images was carried out using FLIRT [44],[50].

C. FNIR Instrument and Sensor

We used a modified frequency-domain spectrophotometer (Oximeter, ISS, Champaign, IL) at two different wavelength,

692 nm and 834 nm. Eight light sources were used, four for each wavelength, and one photomultiplier tube (PMT) detector to collect the light. The output signals from the PMT were sent to a computer for data processing and the AC, DC, and Φ of the wave were determined. The sensor consisted of four source-detector pairs with four sources placed 2 cm and 2.5 cm away from the detector in a symmetric fashion, as shown in Fig. 1.

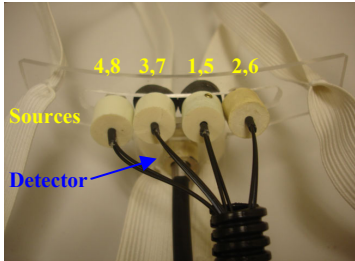


Fig. 1 Actual sensor head design. This straps onto the head at the region determined from the fMRI trial. We used a symmetric sensor head design with one detector and eight sources. Sources 1-4 were 692 nm and 5-8 were 834 nm.

Every two sources (692 nm and 834 nm) were coupled to allow for more accuracy and limit the number of positions to four. The sources and detector were held into place by a plastic molded strap with a slight bend in order to fit comfortably (using elastic straps) on the subject's head.

D. Task

The subject was instructed to fixate eyes for 30 seconds (OFF condition) and then move eyes back and forth in a saccadic fashion for 30 seconds (ON condition). This same task was performed for the fMRI trial. The difference between these two states was calculated.

E. fNIR Data Analysis

The raw AC and DC data were analyzed. However we did not use the algorithm provided by the frequency domain instrument, rather we derived our own computation based on the modified Beer-Lambert law. The raw data was filtered using a moving average. The extinction coefficients for oxyhemoglobin and deoxyhemoglobin were taken from a table. The differential path length factors were derived for both wavelengths [51].

IV. RESULTS

After localizing the visual cortex through the fMRI activation we were able to successfully monitor the corresponding changes in oxyhemoglobin and deoxyhemoglobin as a result of the functional ON-OFF paradigm. Overall the results from the sources from each side were symmetric as expected. The source-detector pairs at 2.5 cm showed a stronger signal than the 2 cm distance. This is expected because the 2 cm does not penetrate as deep as the 2,5 cm distance and thus may not detect the signal as efficiently. The results of the trial are illustrated accordingly, Fig. 2-5.

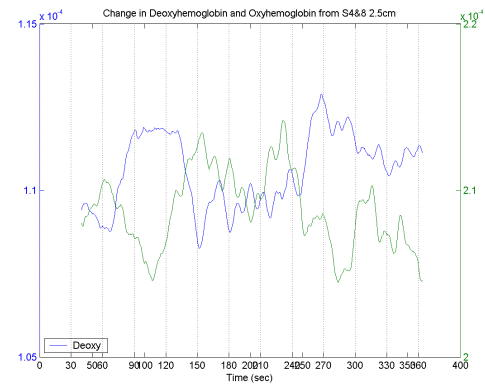


Fig. 2 Relative change in concentration of oxyhemoglobin (HbO) and deoxyhemoglobin (Hb) as a result of alternating between OFF-ON paradigm for sources 4 and 8. The characteristic pattern in the plot shows that as the HbO (blue) increases the Hb (green) decreases.

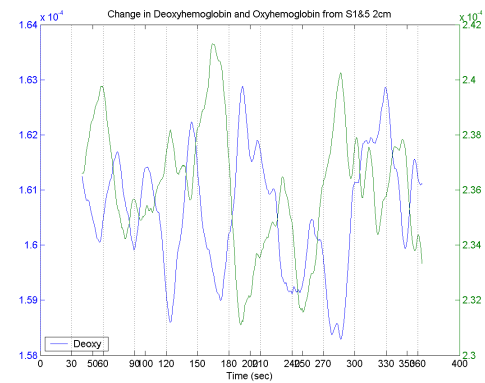


Fig. 3 Relative change in concentration of oxyhemoglobin (HbO) and deoxyhemoglobin (Hb) as a result of alternating between OFF-ON paradigm for sources 1 and 5. The characteristic pattern in the plot shows that as the HbO (blue) increases the Hb (green) decreases.

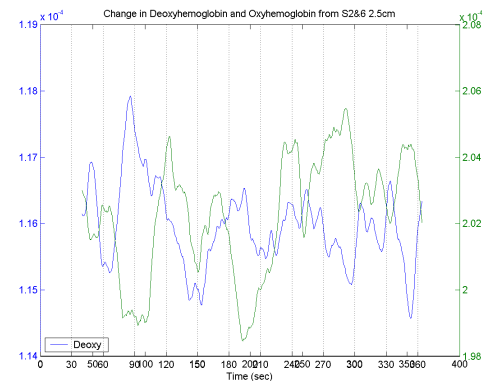


Fig. 4 Relative change in concentration of oxyhemoglobin (HbO) and deoxyhemoglobin (Hb) as a result of alternating between OFF-ON paradigm for sources 2 and 6. The characteristic pattern in the plot shows that as the HbO (blue) increases the Hb (green) decreases.

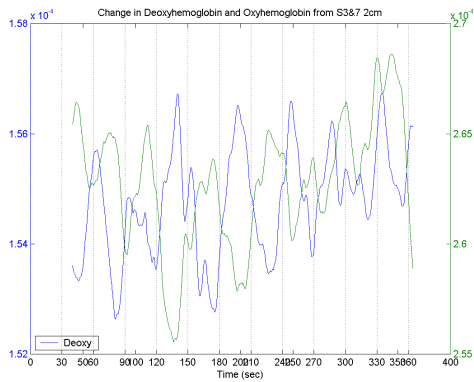


Fig. 5 Relative change in concentration of oxyhemoglobin (HbO) and deoxyhemoglobin (Hb) as a result of alternating between OFF-ON paradigm for sources 3 and 7. The characteristic pattern in the plot shows that as the HbO (blue) increases the Hb (green) decreases.

V. DISCUSSION

FMRI and NIR are complimentary to each other in that they allow for the monitoring and measurement of changes in the oxy to deoxy hemoglobin ratio, which corresponds to activation. While FMRI is well developed, NIR is still lagging behind with respect to imaging the visual cortex and is not ready for the clinical environment. NIR measurement accuracy can vary depending on the design of the detector head. Constant optode distance is crucial; if head circumference changes even by a fraction of a millimeter, the trends are significantly biased [52]. Strangman et al. [53] did a comprehensive study on factors affecting the accuracy of NIR concentration calculations and found that the wavelength selection and optode placement to be important factors in reducing error. A limitation of NIR is its low spatial resolution [54]. Statistical parametric mapping, as in FMRI, cannot be directly applied to NIRS studies because there are too few measurement portions [13]. On the other hand compared to other imaging methods, optical approaches have an excellent temporal resolution [10],[55] that enables analysis in the frequency domain. NIR is also low cost, non-invasive, and portable.

The use of functional MRI has proved to be a successful imaging modality but unfortunately, like many other modalities, it has its drawbacks. The main being cost and portability. Therefore, the development of novel, more selective, and noninvasive diagnostic techniques is a priority. The inherent potential of this optical technique is that it is noninvasive and can be used during behavioral tasks in order to provide temporal and spatial information, making it ideal for infant research [12]. However, this technique is limited by its low spatial resolution. With all these in mind, it is clear that there is a significant clinical need for low cost, non-invasive, portable imaging modalities that combines both high spatial resolution and high physiological sensitivity to improve the clinical sensitivity and specificity for visual cortex (and long term motor cortex) diagnosis.

FNIRS has several advantages in comparison with other imaging methods, such as high flexibility, portability, low cost and biochemical specificity. Moreover, patients and

children who might not stand the confined environment of functional magnetic resonance imaging (FMRI) experiments can be repetitively examined. Therefore, it is useful to further establish FNIRS as a method for functional imaging. NIRS may be useful in detecting visual dysfunction objectively and noninvasively in patients with visual disturbance, especially when used at the bedside [11],[56]. Specifically, Miki et al [11] demonstrated that a decreased activation of the visual cortex in patients with optic neuritis can be seen with NIRS. As for the field of evaluating visual function via the cortex, this has not yet gained popularity. The use of FNIR and FMRI concurrently may lead to new findings in the area of functional imaging. Studies combining FMRI and FNIR are now emerging [1]-[6].

VI. CONCLUSION

We have demonstrated the feasibility of using both FMRI and FNIR in order to localize and monitor visual function. This has potential for a low cost continuous monitoring of visual disorder via FNIR, after an initial diagnosis is made through FMRI.

REFERENCES

- [1] A. Kleinschmidt, H. Obrig, M. Requardt, K. D. Merboldt, U. Dirnagl, A. Villringer and J. Frahm, "Simultaneous Recording of Cerebral Blood Oxygenation Changes During Human Brain Activation by Magnetic Resonance Imaging and Near-Infrared Spectroscopy." *Journal of Cerebral Blood Flow & Metabolism* (1996) 16, 817-826.
- [2] T. J. Huppert, R. D. Hoge, M. A. Franceschini, D. A. Boas, "A spatial-temporal comparison of fMRI and NIRS hemodynamic responses to motor stimuli in adult humans." *Abstract Proceedings of SPIE -- Volume 5693 Optical Tomography and Spectroscopy of Tissue VI*, Britton Chance, Robert R. Alfano, Bruce J. Tromberg, Mamoru Tamura, Eva M. Sevick-Muraca, Editors, April 2005, pp. 191-202.
- [3] X. Zhang, V. Y. Toronov, A. G. Webb, "Spatial and temporal hemodynamic study of human primary visual cortex using simultaneous functional MRI and diffuse optical tomography." *Proc IEEE EMB 727-730 Sep 2005a*.
- [4] X. Zhang, V. Y. Toronov, A. G. Webb, "Simultaneous integrated diffuse optical tomography and functional magnetic resonance imaging of the human brain." *Optics express Vol 13 No 14 5513-21 2005b*.
- [5] M. L. Schroeter, M. M. Bucheler, R. Scheid, "Circadian variability is negligible in primary visual cortices as measured by fNIRS." *Int J Psychophysiol* 62, 9-13 2006a.
- [6] J. Steinbrink, A. Villringer, F. Kempf, D. Haux, S. Boden, H. Obrig, "Illuminating the BOLD signal: combined fMRI-fNIRS studies." *MRI* 24, 495-505 2006.
- [7] H. Obrig, R. Wenzel, M. Kohl, S. Horst, P. Wobst, J. Steinbrink, F. Thomas, and A. Villinger, "Near-infrared spectroscopy: does it function in functional activation studies of adult brain?" *International Journal of Psychophysiology*, 35:125-142, 2000b.
- [8] H. Obrig and A. Villinger, "Beyond the visible-imaging the human brain with light." *Journal Cereb. Blood Flow Metab.*, 23:1-18, 2003.
- [9] G. Strangman, D. A. Boas, and J. P. Sutton, "Non-invasive neuroimaging using near-infrared light." *Biol. Psychiatry*, 52:679-693, 2002a.
- [10] A. Villringer and B. Chance, "Non-invasive optical spectroscopy and imaging of human brain function." *Trends Neurosci.*, 20:435-442, 1997.
- [11] A. Miki, T. Nakajima, M. Takagi, T. Usui, H. Abe, C. S. J. Liu, and G. T. Liu, "Near-infrared spectroscopy of the visual cortex in unilateral optic neuritis." *Am J Ophthalmol*, 139:353-356, 2005.

- [12] T. Wilcox, H. Bortfeld, R. Woods, E. Wruck, and D. A. Boas, "Using near-infrared spectroscopy to assess neural activation during object processing in infants." *Journal of Biomedical Optics*, 10, 2005.
- [13] Y. Hoshi, "Functional near-infrared optical imaging: utility and limitations in human brain mapping." *Psychophysiology*, 40:511-20, 2003.
- [14] M. Ferrari, L. Mottola, and V. Quaresima, "Principles, techniques, and limitations of near infrared spectroscopy." *J Appl Physiol*, 29:463-87, 2004.
- [15] R. P. Kennan, S. G. Horowitz, A. Maki, Y. Yamashita, H. Koizumi and J. C. Gore, "Simultaneous recording of event-related auditory oddball response using transcranial near infrared optical topography and surface EEG." *NeuroImage*, 16:587-592, 2002.
- [16] G. Taga, K. Asakawa, A. Maki, Y. Konishi, and H. Koizumi, "Brain imaging in awake infants by near-infrared optical topography." *PNAS*, 100(19):10722-10727, 2003.
- [17] M. Cope and D. T. Delpy, "System for long-term measurement of cerebral blood flow and tissue oxygenation on newborn infants by infrared transillumination." *Med. Biol. Eng. Comput.*, 26:289, 1988.
- [18] M. Cope, "The development of a near-infrared spectroscopy system and its application for noninvasive monitoring of cerebral blood and tissue oxygenation in the newborn infant." University College London, 1991.
- [19] D. A. Boas, M. A. Franceschini, A. K. Dunn, and G. Strangman, "Noninvasive imaging of cerebral activation with diffuse optical tomography", chapter 8, pages 193-221. CRC Press, 2002.
- [20] J. C. Hebden, S. R. Arridge, and D. T. Delpy, "Optical imaging in medicine: I. experimental techniques." *Phys. Med. Biol.*, 42:825, 1997.
- [21] D. A. Benaron and D. K. Stevenson, "Optical time-of-flight and absorbance imaging of biologic media." *Science*, 259:1463, 1993.
- [22] B. Chance and et al. "Comparison of time-resolved and unresolved measurements of deoxyhemoglobin in brain." In *Proc Natl Acad Sci USA*, 85, page 4971, 1988.
- [23] R. Cubeddu and et al. "Time-resolved imaging on a realistic tissue phantom: us' and ua images vs. time-integrated images." *Appl. Opt.*, 35:4533, 1996.
- [24] D. Grosenick, H. Wabnitz, and H. Rinneberg, "Time-resolved imaging of solid phantoms for optical mammography." *Appl. Optics*, 36:221, 1997.
- [25] J. C. Hebden, "Evaluating the spatial resolution performance of a time-resolved optical imaging system." *Med. Phys.*, 19:1081, 1992.
- [26] E. Gratton and et al. "Measurements of scattering and absorption changes in muscle and brain." *Philos. Trans. R. Soc. Lond. B Biol. Sci.*, 352:727, 1997.
- [27] H. Jiang and et al. "Simultaneous reconstruction of optical absorption and scattering maps in turbid media from near-infrared frequency-domain data." *Opt. Lett.*, 20:2128, 1995.
- [28] B. W. Pogue and M. S. Patterson, "Frequency-domain optical-absorption spectroscopy of finite tissue volumes using diffusion-theory." *Phys. Med. Biol.*, 39:1157, 1994.
- [29] B. W. Pogue and M. S. Patterson, "Instrumentation and design of a frequency-domain diffuse optical tomography imager for breast cancer detection." *Optics Express*, 1:391, 1997.
- [30] S. Nioka, Q. Luo, and B. Chance, "Human brain functional imaging with reflectance cws." *Adv. Exp. Med. Biol.*, 428:237, 1997.
- [31] A. M. Siegel, J. J. A. Marota, and D. A. Boas, "Design and evaluation of a continuous wave diffuse optical tomography system." *Optics Express*, 4:287, 1999.
- [32] A. Maki and et al. "Visualizing human motor activity by using non-invasive optical topography." *Front Med. Biol. Eng.*, 7:285, 1996.
- [33] W. Colier and et al. "A new and highly sensitive optical brain imager with 50 hz sample rate." *NeuroImage*, 11:542, 2000.
- [34] A. P. Gibson, J. C. Hebden, and S. R. Arridge, "Recent advances in diffuse optical imaging." *Phys. Med. Biol.*, 50, 2005.
- [35] S. R. Arridge and W. R. B. Lionheart, "Nonuniqueness in diffusion-based optical tomography." *Optics Lett.*, 23:882, 1998.
- [36] S. R. Arridge, "Photon measurement density functions: I. analytical forms." *Appl. Opt.*, 34:7395-409, 1995.
- [37] S. R. Arridge and M. Schweiger, "Photon measurement density functions: II. Finite element method calculations." *Appl. Opt.*, 34:8026-37, 1995.
- [38] K. K. Kwong, J. W. Belliveau, D. A. Chesler, I. E. Goldberg, R. M. Weisskoff, B. P. Poncelet, D. N. Kennedy, B. E. Hoppel, M. S. Cohen, R. Turner, et al. "Dynamic magnetic resonance imaging of human brain activity during primary sensory stimulation." *Proc Natl Acad Sci USA* 89:5675-5679, 1992.
- [39] H. Nakahara, T. Murofushi, "Congenital-type nystagmus in Arnold-Chiari malformation" *Otolaryngol Head Neck Surg* 128:598-600, 2003.
- [40] T. P. Naidich, A. G. Valavanis, A. Kubik, "Anatomic relationships along the low-middle convexity. I. Normal specimens and magnetic resonance imaging." *Neurosurgery* 36:517-532, 1995.
- [41] T. P. Naidich, T. C. Brightbill, "Systems for localizing frontalparietal gyri and sulci on axial CT and MRI." *Int J Neuroradiol* 2:313-338, 1996.
- [42] T. A. Yousry, G. Fesl, A. Buttner, S. Noachtar, U. D. Schmid, "Heschl's gyrus: anatomic description and methods of identification in MRI." *Int J Neuroradiol* 3:2-12, 1997.
- [43] J. Talairach, P. Tournoux, "Co-planar stereotaxic atlas of the human brain." Thieme, Stuttgart, 1988.
- [44] M. Jenkinson, P. Bannister, M. Brady, S. Smith, "Improved optimisation for the robust and accurate linear registration and motion correction of brain images." *NeuroImage* 17:825-841, 2002.
- [45] C. F. Beckmann, S. M. Smith, "Probabilistic Independent Component Analysis for Functional Magnetic Resonance Imaging." *IEEE Trans. on Medical Imaging* 23:137-152, 2004.
- [46] M. W. Woolrich, B. D. Ripley, J. M. Brady, S. M. Smith, "Temporal Autocorrelation in Univariate Linear Modelling of FMRI Data." *NeuroImage* 14: 1370-1386, 2001.
- [47] S. D. Forman, J. D. Cohen, M. Fitzgerald, W. F. Eddy, M. A. Mintun, D. C. Noll, "Improved assessment of significant activation in functional magnetic resonance imaging (fMRI): use of a cluster-size threshold." *Magn Reson Med*.33:636-47, 1995.
- [48] K. J. Friston, G. Tononi, G. N. Reeke Jr, O. Sporns, G. M. Edelman, "Value dependent selection in the brain: simulation in a synthetic neural model." *Neuroscience* 59:229-43, 1994.
- [49] K. J. Worsley, A. C. Evans, S. Marrett, P. Neelin, "A three-dimensional statistical analysis for CBF activation studies in human brain." *J Cereb Blood Flow Metab* 12:900-18, 1992.
- [50] M. Jenkinson, S. M. Smith, "A Global Optimisation Method for Robust Affine Registration of Brain Images." *Medical Image Analysis*.5:143-156, 2001.
- [51] A. Duncan, J. H. Meek, M. Clemence, C. E. Elwell, L. Tyszczuk, M. Cope, and D. T. Delpy, "Optical pathlength measurements on adult head, calf and forearm and the head of the newborn infant using phase resolved optical spectroscopy." *Phys. Med. Biol.* 40:295-304, 1995.
- [52] G. Greisen, "Is near infrared spectroscopy living up to its promises?" *Seminars in Fetal & Neonatal Medicine* 11, 498-502 2006.
- [53] G. Strangman, M. A. Franceschini, and D. Boas, "Factors affecting the accuracy of near-infrared spectroscopy concentration calculations for focal changes in oxygenation parameters." *NeuroImage* 18: 865-879, 2003.
- [54] R. Nossal, A. H. Gandjbakhche and R. F. Bonner, "Resolution limits for optical transillumination of abnormalities deeply embedded in tissues." *Med. Phys.*, 21:185-91, 1994.
- [55] N. Pouratian, S. A. Sheth, N. A. Martin, and A. W. Toga, "Shedding light on brain mapping: advances in human optical imaging." *Trends Neurosci.*, 26:277-282, 2003.
- [56] S. R. Hintz, D. A. Benaron, A. M. Siedel, A. Zourabian, D. K. Stevenson, and D. A. Boas, "Bedside functional imaging of the premature infant brain during passive motor activation." *J. Perinat. Med.*, 29:335-343, 2001.